Response of "The Important Contribution of Secondary Formation and Biomass Burning to Oxidized Organic Nitrogen (OON) in a Polluted Urban Area: Insights from In Situ FIGAERO-CIMS Measurements" in *Atmos. Chem. Phys. Discuss. Doi: 10.5194/acp-2023-8*

Anonymous Referee #1

1.0. This study deploys an AMS and a FIGAERO-CIMS to investigate the sources and formation mechanisms of oxidized organic nitrogen (OON) species in an urban site in Guangzhou, China. By applying a tracer based method to FIGAERO-CIMS measurement, the contributions from biomass burning and secondary production to OON have been quantified. Further, the production rate of secondary OON is estimated based on the measured VOCs concentrations and literature values of ON yields. Overall, this study presents an interesting dataset and conducts comprehensive analysis. It improves our understanding of the concentration and speciation of OON in diverse environments. However, the conclusions on the source apportionment and formation mechanisms of OON are speculative as outlined below. I recommend accept with major revisions noted.

A1.0: We greatly appreciate the reviewer providing the valuable comments and constructive suggestions which help us tremendously in improving the quality of our work. All the responses to the specific comments are shown below. To facilitate the review process, we have copied the reviewer comments in black text. Our responses are in regular blue font. We have responded to all the referee comments and made alterations to our paper **(in bold text).**

Major Comments

1.1. The mass closure analysis on particle OON measured by CIMS and by AMS is valuable. It is shown that pOrgNO3,CIMS only accounts for ~30% of pOrgNO3,AMS (Line 228). In other words, CIMS only captures a small fraction of total pON, if the AMS measurement is reliable. Thus, the majority of the analysis in this study only focuses on a small fraction of total ON. A more important question is what the rest 70% of particle OON are. The reviewer understands this question is beyond the scope of this study, but this measurement limitation should be stressed more throughout the manuscript, to avoid the fallacy that the OON measured by I- CIMS, such as figure 7, represents the composition of all OON in the atmosphere. Similarly, the conclusions like half of particle OON originates from

biomass burning and the rest from secondary production should be discussed under the frame that the OON measured by I- CIMS are considered in the calculation, not total OON in the atmosphere.

A1.1: We agree with the reviewer's comment that the source apportionment results from CIMS cannot represent all the particle- and gas-phase OON in the ambient air. We stressed the measurement limitation of the CIMS throughout the revised main manuscript by emphasizing the OON reported here was mainly applicable to CIMS measurement and the OON mass detected by CIMS only accounted for 30% of values by AMS. For examples:

Line 375-377: **"On average, biomass burning emissions accounted for 49 ± 23% of total pOON measured by the CIMS, while the contribution was much lower (24 ± 25%) for gOON (Figs. 2b and 2d), indicating that biomass burning is one of the major sources for pOON measured by the CIMS, and gOON is predominately from secondary formation (76 ± 25%) (Huang et al., 2019; Lee et al., 2016)."**

Line 496-497: **"In this section, the molecular components of the gOON and pOON measured by the CIMS categorized with different oxygen and carbon atom numbers are briefly discussed."**

Line 534-535: **"Note that the sources of the undetected pOON from CIMS are still unknown, which shall be further investigated."**

Please also note that although the pOON measured by the CIMS only accounts for ~30% of the mass loading measured from AMS, we found that the measured pOON from two techniques correlated well, suggesting the rest of ~70% of mass from CIMS may have similar variation. Per reviewer #2's comments, we also calculated the potential uncertainty of measured pOON between CIMS and AMS. We found that the $pOrgNO_{3,CIMS}$ accounted for 28 ± 18% of $pOrgNO_{3,AMS}$ combined with uncertainty analysis in the revised Text S3 in supporting in formation. The detailed calculation can be found in A2.5.

1.2. Using C6H10O5I- as a tracer for biomass burning is not adequately justified. A major piece of evidence that biomass burning contributes to OON is figure 2a and 2c, which show the relationship between OON and C6H10O5I- is bifurcated. However, the same relationship is not observed between OON and other BB tracers including AMS mz60, methoxyphenol, and vanillic aicd. The contrasting observations are suspicious. The manuscript claims that BB tracers other than levoglucosan have all sorts of issues, such as non-biomass burning emissions, low concentration, or larger background. These issues could certainly be true. However, an obvious issue with C6H10O5I- is that it is not solely levoglucosan, but has interference from other isomers! Thus, it can be easily argued that C6H10O5I- is not a perfect tracer either. One should not rely the analysis solely on this single chemical formula. Let's imagine, among all the

CIMS ions, one ion, which is a tracer for VCP for example, exhibits similar correlation relationship with OON as C6H10O5 does (i.e., bifurcation as in Figure 2a). Then, the conclusion will easily become that VCP is a large contributor to OON. In conclusion, more evidence is required to support the contribution of biomass burning to OON. The authors mentioned that there are some episodes when pOON and levoglucosan peak coincidently (Figures S11a and S12a). Again, the figures only show pOON has some relationship with C6H10O5I-, not with levoglucosan, because the C6H10O5I- could be some other isomers.

A1.2: As the reviewer mentioned that the formula $C_6H_{10}O_5$ consisted of isomers in ambient atmosphere, which are levoglucosan, mannosan, and galactosan. In the same campaign, we also measured the isomer of levoglucosan based on filter sampling analyzed by high performance anion exchange chromatography with pulsed amperometric detection (HPAEC-PAD) (Zhang et al. 2015). The detailed information about this measurement can be found in recently published paper of Jiang et al. (2023) in the Science of Total Environment journal. The isomer measurement showed that the levoglucosan contributed 90 ± 2% of the total mass loading from three isomers of $C_6H_{10}O_5$ (Fig. A1) through the campaign, which was consistent with the previously reported results across China (80−95%) (Mao et al., 2018; Ho et al., 2014; Müller et al., 2023; Wang et al., 2018; Zhu et al., 2020).

Furthermore, we added measured results of potassium (K^+) to verify the source of $C_6H_{10}O_5$. K^+ can be treated as a tracer for biomass burning (Wang et al., 2017; Andreae, 1983) and is detected using IC based on filter sampling. The consistent variation of potassium (K^+) and levoglucosan supported that the enhancement of $C_6H_{10}O_5$ at high mass concentration shall mainly come from biomass burning (Wang et al., 2017), as shown in the reproduced Fig. S11a below.

To clarify this, we added corresponding information and revised the description in line 179-183 in the maintext as below. To be more precise and avoid confusion, we also updated all the compound name "**levoglucosan**" to be "**$C_6H_{10}O_5$**" or "**$C_6H_{10}O_5$ (levoglucosan and its isomers)**" when CIMS measurement was referred to in the manuscript. The uncertainty of using $C_6H_{10}O_5$ as tracer for biomass burning source apportionment of OON was also added, the detailed information can be found in A2.10.

"In the ambient air, the $C_6H_{10}O_5$ measured in the particle phase using the CIMS was probably composed by levoglucosan and its isomers (mannosan and galactosan) (Ye et al., 2021). The isomer measurement of $C_6H_{10}O_5$ in this campaign have revealed that the levoglucosan contributed 90 ± 2% mass loading of the three isomers of $C_6H_{10}O_5$ (Jiang et al., 2023), thus the $C_6H_{10}O_5$ signal in this study can be used as a tracer for biomass burning

emission (Bhattarai et al., 2019). The good correlation (R=0.78) between $C_6H_{10}O_5$ and another biomass burning tracer potassium (K^+) (Wang et al., 2017; Andreae, 1983), also supports this statement (Fig. S11a)."

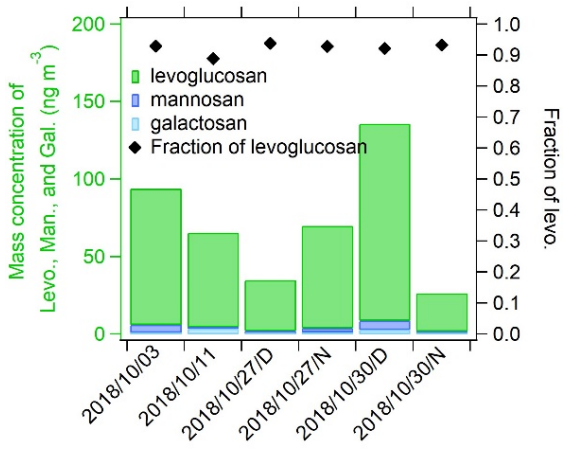

Figure A1. The mass concentration of $C_6H_{10}O_5$ isomers, i.e., levoglucosan, mannosan, and galactosan in this campaign. The mass fraction of levoglucosan to total $C_6H_{10}O_5$ isomer mass loading is also shown.

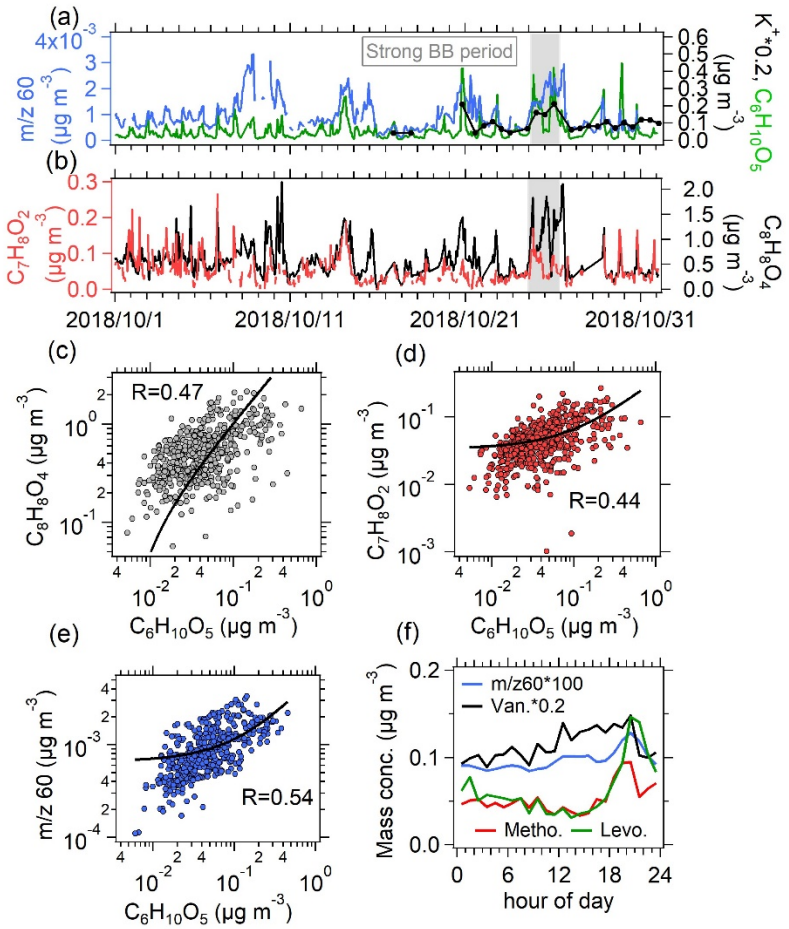

Figure S11. (a) Time series of *m/z* 60 from the AMS, particulate $C_6H_{10}O_5$ (levoglucosan and its isomers), water-soluble potassium (K^+), (b) $C_7H_8O_2$ (methoxyphenol and its isomers) and $C_7H_8O_2$ (methoxyphenol and its isomers) from CIMS. The *m/z* 60 was found to be a fragment from levoglucosan-like species and supposed to

be a tracer of biomass burning (Cubison et al., 2011). Scatter plots of (c) $C_7H_8O_2$ (methoxyphenol and its isomers), (d) $C_8H_8O_4$ (vanillic acid and its isomers), and (e) *m/z* 60 versus levoglucosan. Moderate agreement between them and $C_6H_{10}O_5$ also demonstrates the existence of biomass burning emissions (Urban et al., 2012). (f) Diurnal variation of the four species.

1.3. The production rate of secondary OON is estimated based on measured VOCs, but the usefulness of this analysis is limited. First, as the OON concentration depends on both production and loss, which is clearly pointed out in Line 369-371, the correlation between OON concentration and product rate is not very meaningful. As a result, there is no clear correlation between two terms as shown in this study. Second, the calculated production rate is not tied to the I CIMS measurement, which degrades the importance of such analysis. In other words, both methods do not validate each other. But it is at the authors' discretion regarding whether to keep this analysis.

A1.3: The production rate of OON was widely applied to investigate the formation pathway and potential contribution of VOCs to OON (Rollins et al., 2012; Liebmann et al., 2019; Sobanski et al., 2017; Ayres et al., 2015; Perring et al., 2013; Hamilton et al., 2021; Pye et al., 2015). It is true that the production rate did not account for the loss of OON results, however, to properly simulate the ambient OON concentration need modeling work with detailed mechanism account for the extra loss pathways including oxidation, photolysis, hydrolysis and deposition. The model simulation on mass concentration of OON in urban areas is still a challenge due to the complex formation and loss way of anthropogenic-derived OON (Li et al., 2023), which is beyond the scope of this manuscript. Under such background, the production rate calculation itself would be very meaningful to explore the formation mechanism of OON in urban areas in preliminary. In this study, we estimated the ambient mass concentration of NO_3 radicals based direct measurement of N_2O_5 by CIMS and obtained the time series of OH mass concentration using MCM model constrained by real J-value measurement. The detection of VOCs was also validated with multiple techniques. Overall, the dataset used for production rate estimation here is in high quality. Considering the uncertainty in both measurement of secondary gOON by CIMS and estimation of OON production rate, their similar diurnal variations show good agreement, which also supports the reasonability of the production rate calculated here. The rate production results give a summarized overview for the OON formation pathways and help us to better understand the future focus of OON studies. E.g., through OON production rate calculation, we found important OON formation through NO_3 pathways during the daytime, which highlight the potential contribution of NO_3 oxidation to other secondary products, e.g., SOA . The important contribution from monoterpene oxidation to OON was also revealed. Thus, we would like to keep these results and believe it is a very important part of our study. Finally, we revised the sentences in line 414-417 to remind the readers the potential uncertainty of production rate calculation in the maintext:

"To further elucidate the secondary formation mechanism of gOON, the diurnal patterns of gOON production rates from the three pathways following the procedure mentioned in section 2.3 are calculated and shown in Fig. 4a and Fig. S21. Although the production rate did not consider the loss of OON, the calculation of production rate still serves as a useful tool to assess the formation pathway and precursor contribution to OON (Liebmann et al., 2019; Sobanski et al., 2017; Hamilton et al., 2021)."

We also remind the readers that the life of pOON accounting for the loss of pOON shall be further investigated in the future in line 493-494:

"For the lifetime of pOON, a modeling study including explicit formation mechanism as conducted by Lee et al. (2016) is required for systematic explorations in the future."

1.4. Even though some analysis methods have been used in the literature, they still should be briefly explained to guide the readers who are not familiar with the methods. For example, Line 155 – 158 mentioned that three methods are applied to estimate the ON concentration based on AMS measurements. The basic principles behind each method should be briefly discussed (i.e., one or two sentences). For example, the NO2+/NO+ ratio method is based on the fact that inorganic and organic nitrates have different fragmentation patterns. Another examples include Line 232 and seasonal decomposed analysis (Line 348). Please briefly discuss the methods. Lastly, Line 431, please explain how the lifetime of gON is estimated.

A1.4: The detailed description of the three methods that were applied to estimate the ON concentration was already presented in detail in section 1 of the supporting information, where the principle of three ON estimation methods based on AMS measurement and the calculation process were fully addressed. Per the reviewer's comment, we also added brief description of each method in the revised main text in line 195-201:

"In addition to the total organic aerosol (OA), the mass concentration of $-ONO_2$ group from pON ($pOrgNO_{3,AMS}$) was also estimated by NO_2^+/NO^+ ratio method (Farmer et al., 2010; Fry et al., 2013; Day et al., 2022; Xu et al., 2015), positive matrix factorization (PMF) method (Hao et al., 2014), and thermodenuder (TD) method (Xu et al., 2021b) based on the AMS data. The NO_2^+/NO^+ ratio method was based on the different ratios of NO_2^+ to NO^+ fragmented from $pOrgNO_{3,AMS}$ and inorganic nitrate. The PMF method was performed by including the NO^+ and NO_2^+ ions into the PMF analysis combined with spectral matrix of organic ions. The TD method was conducted based on the difference of volatility between $pOrgNO_{3,AMS}$ and inorganic nitrates in particles."

The revised explanation of seasonal decomposed analysis can refer to Text S4 in supporting information manuscript. We also added brief description of the method and revised the sentence in the revised main text in line 400-403:

"To elucidate this large uncertainty, a seasonal decomposition method (Hilas et al., 2006), which was performed by locally weighted linear regression to decompose the time series into three components, i.e., trend component, seasonal component and remainder, was applied (detailed process can be found in Text S4). By replacing seasonal variation with hour variation, the method can down weight the impact of daily peak intensity variation."

We revised the estimation method of the lifetime of gOON in the last paragraph of section 3.3 (line 487-489):

"Furthermore, the lifetime of gOON in this study can be approximately estimated by a steady-state approach (gOON mixing ratio versus total production rate) as shown in Liebmann et al. (2019). A scatterplot of the secondary gOON versus the secondary gOON production rate at 1 hour time resolution is shown in Fig. S24b."

1.5. Issues regarding CIMS quantification. Does the calibration account for the temperature-dependence? A recent study shows that the I- CIMS sensitivity has a strong dependence on temperature[1]. This issue could be significant for particle-phase measurements, which have a higher IMR temperature. Line 134 mentioned that a voltage scanning procedure was used to estimate the sensitivity. However, neither detailed procedures nor calibration results are shown. Please describe the procedure, show the calibration curves, and show the accuracy of this method to the 39 compounds calibrated with authentic standards. Please discuss how the calibration curve is applied to estimate the sensitivity of individual compounds. Also, two recent studies have quantified the uncertainty of the voltage scanning method[2, 3], which should be cited and discussed in the manuscript.

A1.5: We thank the reviewer for his/her comments and suggestions. We maintained the IMR temperature in a stable condition by keeping heater strip and room temperature constant, as well as adding an insulation layer outside of the gas sampling line. The temperature of the IMR during measurement was kept almost constant (80 **℃)** to minimize the effect of temperature on sensitivity throughout the experiment set up. Thus, we think the temperature-dependent sensitivity shall be minor in this study. To clarify this, we added relative description in line 127-131 in the revised main text:

"The temperature of the IMR was kept almost constant by setting the temperature constant (80 ℃) of the heater strip in the IMR. Meanwhile, the room temperature, which was maintained by an air-conditioner, was

relatively stable (23.7 ± 2.9 °C). The gas sampling line inside the room was covered by heat insulation associated with a heating cable to hold the temperature of sampling gas steady. These protocols reduce the effect of the temperature dependence of IMR, as indicated by Robinson et al. (2022) that I^- CIMS sensitivity may be influenced by the temperature of IMR."

The detail description of the calibration experiments and data processing in this campaign, e.g., voltage scanning, was already shown in a previous paper of Ye et al. (2021) (copied as Fig. A2 below). We added a brief description on the calibration method about voltage scanning method and how the calibration curve was applied to estimate the sensitivity of individual compound in line 148-160 in the maintext:

" Lopez-Hilfiker et al. (2016) and Iyer et al. (2016) have verified the connections among the binding energy of the iodide-adduct bond, the voltage dissociating iodide adducts and the sensitivity of corresponding species. The relationship between the voltage difference (*dV*) and signal fraction remaining of an iodide-molecule adduct is established by scanning the *dV* between the skimmer of the first quadrupole and the entrance to the second quadrupole ion guide of the mass spectrometer. This relationship curve of an individual iodide adduct can be fitted by a sigmoid function and yields two parameters: S_0, the relative signal at the weakest *dV* compared to the signal under operational *dV*; dV_{50}, the voltage at which half of the maximum signal is removed (i.e., half the adducts that could be formed are de-clustered). A sigmoidal fit was then applied to the results of all the iodide adducts. An empirical relationship between relative sensitivity ($1/S_0$) and dV_{50} of each ion (includes levoglucosan) based on average values of the entire campaign was obtained. By linking the relative sensitivity of levoglucosan with its absolute sensitivity based on the authentic standard, the absolute sensitivity of all the uncalibrated OON species was determined, after taking into account the relative transmission efficient of all the ions. The detailed data of these response factors can be found in the supporting information of Ye et al. (2021)."

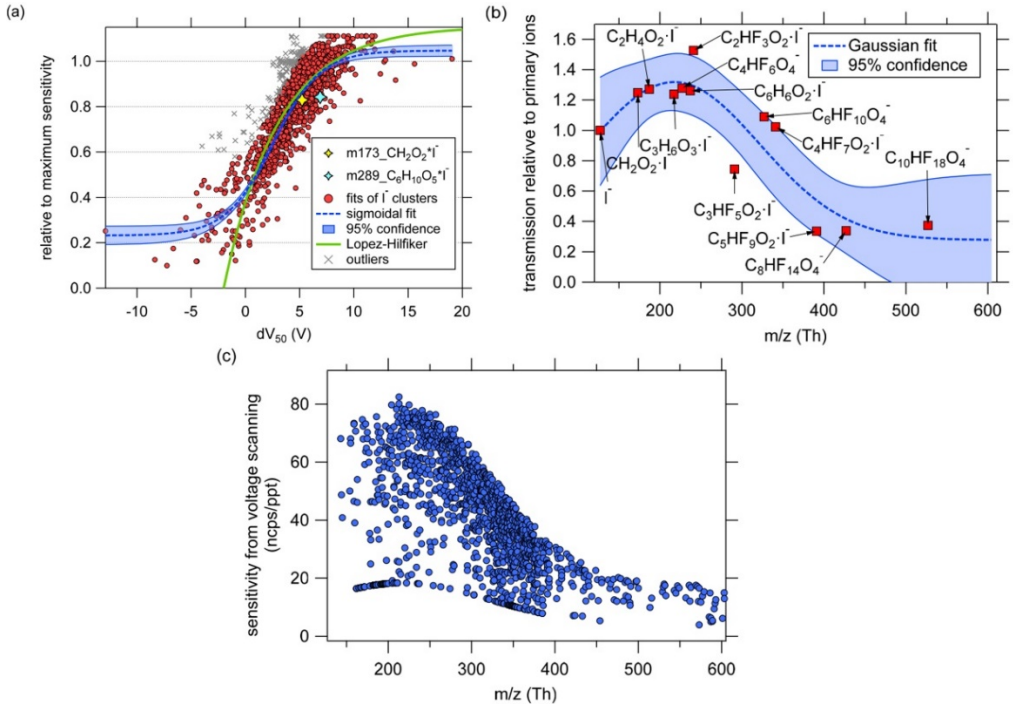

"Figure A2. The original Figure S7 in the supporting information of Ye et al. 2021. (a) Fitting the voltage scanning results as a sigmoidal function of sensitivity relative to maximum sensitivity versus dV_{50} (i.e., the voltage where half of an iodide adducts dissociate). (b) Fitting relative transmission efficiency as a gaussian curve of m/z. (c) The sensitivity derived from voltage scanning procedure. The transmission correction has been applied. The bottom line in Figure A2c that has a shape exactly the same as the transmission curve represents the points with a cutoff of 0.23 for the relative sensitivity."

The uncertainty of voltage scanning method was quantified in previous studies including two studies mentioned by the reviewer and Isaacman-Vanwertz et al. (2018). This approach was found to carry high uncertainties for individual analytes (0.5 to 1 order of magnitude) but represent a central tendency that can be used to estimate the sum of analytes with reasonable error (~30% differences between predicted and measured moles) (Bi et al., 2021b). Based on the analysis of the uncertainties of three nitrogen-containing compounds (in the list of calibrated species) derived both from the voltage scanning method and the method using the standard compounds, we approximately obtained 32–56% underestimation of sensitivity for the voltage scanning method. Through the comparison of the sensitivity factors derived from the two methods is added in Figure S3 (also shown as below), an average value of 47% was regarded as the uncertainty of the voltage scanning method and the total mass loading of uncalibrated species. To clarify this, we added the description of uncertainty analysis of the voltage scanning method in line 160-168:

"Three OON species which are 4-nitrophenol ($C_6H_5NO_3$), 2,4-dinitrophenol ($C_6H_4N_2O_5$), and 4-nitrocatechol ($C_6H_5NO_4$) were calibrated in both authentic standards and voltage scanning methods. By comparing their sensitivity (Fig. S3), the uncertainty of the voltage scanning method can be roughly estimated. Detailed description of the calibration curves and the application of the calibration curve to estimate the sensitivity can

be referred to the supporting information text of Ye et al. (2021). In general, the voltage scanning method underestimates (32−56%) the sensitivity of OON in this study compared to the values using the standard compounds as real. This uncertainty was comparable with 30% uncertainty of all analytes in Bi et al. (2021b) and 60% uncertainty of total carbon in Isaacman-Vanwertz et al. (2018) measured by the Iodide-CIMS. Finally, an avergae underestimation of 47% on sensitivity was taken as the uncertainty of the whole OON mass loading in this study."

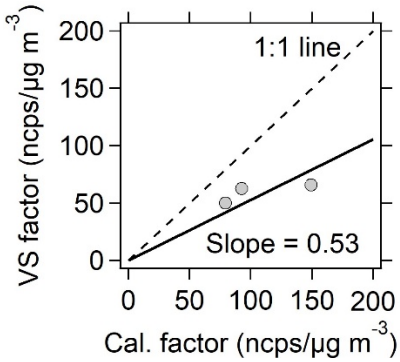

Figure S3. The scatterplot of calibration factors of three nitro-containing compounds (4-nitrophenol, 2,4-dinitrophenol, and 4-nitrocatechol) that derived from voltage scanning method and standard calibration. Based on the slope, 47% was regarded as the uncertainty of the voltage scanning method for OON calibration in this study. The detailed data can be found in the excel file of the supplement zip package of Ye et al. (2021).

Minor Comments

1.6. Lines 50 and 78. Please cite Xu et al. 2015 ACP4 which also extensively discussed the NO2+/NO+ ratio method.

A1.6: In fact, the paper Xu et al. 2015 ACP was already cited in line 204 in the original main text and also in Text S1 in the supporting information. After checking through the manuscript, we also added the citation of Xu et al. 2015 ACP in Line 50, line 78 and line 194 in the revised main text:

In line 50: **"(II) by using aerosol mass spectrometer (AMS) (Decarlo et al., 2006) based on NO_2^+/NO^+ apportionment (Farmer et al., 2010; Fry et al., 2013; Hao et al., 2014; Day et al., 2022; Xu et al., 2015) and/or thermodenuder (Xu et al., 2021b);"**

In line 78: **"Previous studies indicated that the oxidation of biogenic VOCs by NO_3 dominated gOON formation at a forest-urban site in Germany (56% of average gOON production rate) (Sobanski et al., 2017), as well as at a boreal forest site in the Finland (70% of total gOON production rate) (Liebmann et al., 2019) and the southeast US (84% of monoterpene organic nitrate mass) (Ayres et al., 2015; Pye et al., 2015; Xu et al., 2015)."**

In line 197: **"In addition to the total organic aerosol (OA), the mass concentration of $-ONO_2$ group from pON ($pOrgNO_{3,\ AMS}$) was also estimated by NO_2^+/NO^+ ratio method (Farmer et al., 2010; Fry et al., 2013; Day et al., 2022; Xu et al., 2015),"**

1.7. Line 60. Please cite Chen et al. 2020 ACP5 which also deployed FIGAERO-CIMS to measure organic nitrates. Please also discuss Chen et al. in related analysis, such as the comparison between AMS and FIGAERO-CIMS.

A1.7: We thank the reviewer for the reminding. We have read attentively through the paper of Chen et al. 2020 ACP, then added the citation of Chen et al. (2020) in the corresponding sentence in line 61 and in the overview of pON/OA in Fig. S7 as shown below.

"So far, gOON and pOON (containing 4–12 oxygen atoms) formed from multiple oxidation process of volatile organic compounds (VOCs) have been quantified by a high-resolution time-of-flight CIMS installed with a Filter Inlet for Gases and AEROsols (FIGAERO-CIMS) in the forests (Lee et al., 2018; Lee et al., 2016) and at rural sites (Huang et al., 2019; Chen et al., 2020)."

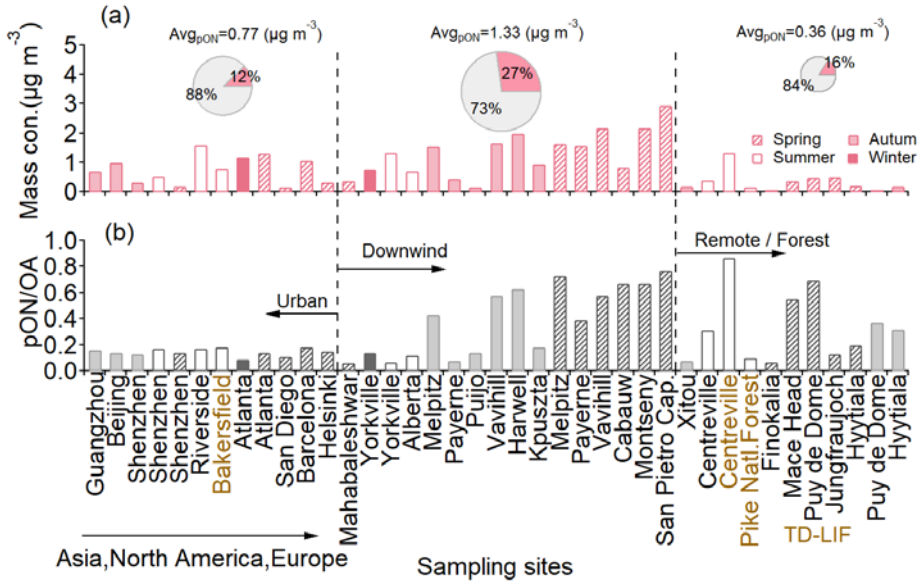

Figure S7. (a) Mass concentration pON and (b) its fraction to OA at sites around the world (Ayres et al., 2015; Chen et al., 2020; Day et al., 2010; Farmer et al., 2010; Fisher et al., 2016; Fry et al., 2013; Kiendler-Scharr et al., 2016; Lanz et al., 2010; Lee et al., 2019; Rollins et al., 2012; Salvador et al., 2020; Singla et al., 2019; Xu et al., 2015; Yu et al., 2019) classified into urban sites, downwind sites (lied downwind of the cities where were influenced by the emissions from the cities), forest or remote sites with different seasons. The average molecular weight of ON used for all sites is assumed to be 200 g mol^{-1}. The inset pies indicate the average fraction of pON

(pink) to OA at each type of site. The yellow indicates the data are measured by thermal dissociation laser-induced fluorescence instrument (TD-LIF). The method of the $pON_{AMS/TD-LIF}$/OA calculation was referred to Takeuchi and Ng (2019).

1.8. Line 125. Do all 339 compounds have signal significantly higher than the background? Or 339 refers to the number compounds that are fitted in the HR analysis?

A1.8: Yes, the 339 compounds were selected due to that they can be fitted in the HR analysis after subtracting the background. To clarify this, we revised the sentence in line 138-140.

"Based on the CIMS measurement, speciated OON (nitrogen-containing oxygenated hydrocarbons, 339 closed-shell compounds with oxygen versus carbon atom ratio no less than 3, $C_{\geq 1}H_{\geq 1}O_{\geq 3}N_{1-2}$) in both gas and particle phases were quantified. These OON compounds can be fitted well in the HR analysis after the background signals have been removed."

1.9. Line 200. The underlying assumption of this statement is unclear. Does the fraction of organic nitrate in total nitrate increases with decreasing OA concentration?

A1.9: We are sorry that we do not quite understand what the assumption that the reviewer refers to here. For the second question, the fraction of organic nitrate in total nitrate as a function of OA concentration was displayed in Fig. A3. The faction of ON in total nitrates decreases as a function of OA mass concentrations above 10 μg m^{-3}.

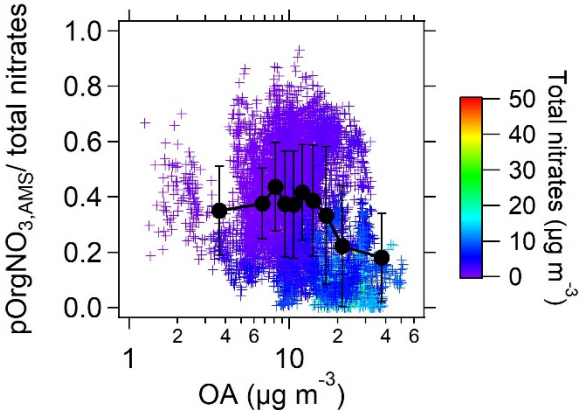

Figure A3. Mass fraction of $pOrgNO_{3,AMS}$ (NO_2^+/NO^+ ratio method) to total nitrates as a function of total OA derived from the AMS. The points are color-coded with total nitrates.

1.10. Line 225-228. There are many acronyms in this paragraph, including $pOON_{CIMS}$, $pOON_{AMS}$, $pOrgNO3_{CIMS}$, $pOrgNO3_{AMS}$. Please better explain the difference between these terms.

A1.10: To provide a comprehensive explanation of the acronyms, we added Table A1 in the appendix to explain all nomenclature mentioned in this manuscript:

"Appendices A: Summary of the acronym

Table A1. The summary of the acronym and corresponding full name in this study.

Acronym	Full name	Acronym	Full name
ALWC	aerosol liquid water content	ONs	organic nitrates
$C_{11-20}N$	oxidized organic nitrogen molecules with 11−20 carbon atoms	OON	oxidized organic nitrogen
$C_{4-5}N$	oxidized organic nitrogen molecules with 4−5 carbon atoms	OON_{bb}	oxidized organic nitrogen from biomass burning
$C_{6-9\ Aro}N$	oxidized organic nitrogen molecules with 6−9 carbon atoms and benzene ring	OON_{sec}	oxidized organic nitrogen from secondary formation
$C_{8-10}N$	oxidized organic nitrogen molecules with 8−10 carbon atoms	O_x	odd oxygen, sum of O_3 and NO_2
CHON	oxidized organic nitrogen with only one nitrogen atom	pC_xN	particle-phase C_xN
$CHON_2$	oxidized organic nitrogen with two nitrogen atoms	PMF	positive matrix factorization
CIMS	chemical ionization mass spectrometer	pON	particle-phase organic nitrates
$C_{others}N$	oxidized organic nitrogen molecules not in other four group	pOON	particle-phase oxidized organic nitrogen
C_xN	oxidized organic nitrogen molecules with x carbon atoms	$pOON_{AMS}$	particle-phase oxidized organic nitrogen derived from aerosol mass spectrometer measurement.
dV	voltage difference	$pOON_{CIMS}$	particle-phase oxidized organic nitrogen measured by chemical ionization mass spectrometer
dV_{50}	the voltage at which half the signal is removed (i.e., half of iodide adducts dissociate)	$pOrgNO_{3,\ AMS}$	Nitrate functional group from particle-phase OON measured by aerosol mass spectrometer
FIGAERO-I-CIMS	an iodide-adduct chemical ionization mass spectrometer equipped with a Filter Inlet for Gases and AEROsols	$pOrgNO_{3,CIMS}$	Nitrate functional group in particle-phase OON based on the data by chemical ionization mass spectrometer
GC-MS/FID	gas chromatography coupled with mass spectrometry and flame ionization detector	PRIDE-GBA	Particles, Radicals, and Intermediates from oxidation of primary Emissions over the Great Bay Area
gON	gas-phase organic nitrates	PTR-ToF-MS	proton transfer reaction time-of-flight mass spectrometry
gOON	gas-phase oxidized organic nitrogen	RH	relative humidity
$gOON_{CIMS}$	gas-phase oxidized organic nitrogen measured by chemical ionization mass spectrometer	S_0	the relative signal at weakest *dV* compared to the signal under operational *dV*
HR-ToF-AMS	high-resolution time-of-flight aerosol mass spectrometer	TD	thermodenuder
IMR	ion-molecule reaction region	TD-LIF	thermal dissociation laser induced fluorescence
MW	molecular weight	VCP	volatile chemical product
NO_x	Sum of NO and NO_2	VOCs	volatile organic compounds

"

1.11. Line 247-248. Please explain "high susceptibility influenced by temperature".

A1.11: We revised this sentence in line 293-295:

"The slightly poor correlation of $C_{4-5}N$ groups between gas and aerosol phase was probably caused by less partitioning of substantial formed isoprene-oxidized gOON in the daytime to the pOON compared to other long-chain compounds."

1.12. Line 253. "photolysis rate" in this sentence is confusing, because reader may think it refers to the photolysis rate of OON. Replace "photolysis rate" with jNO2 or solar radiation.

A1.12: "Photolysis rate" was replaced with "jNO_2" in line 300.

1.13. Line 258. It should be figure 1d, instead of figure 1f.

A1.13: Corrected (in line 305).

1.14. Line 282. replace "NO/NOx concentration" with "NO and NOx concentrations".

A1.14: Corrected (in line 330).

1.15. Line 312 and Text S4. If the reviewer understands correctly, the "seasonal decompose analysis" removes the seasonal variation from the diurnal variation. However, the data only include one-month measurement and it is not clear why this analysis is necessary. Also, text S4 does not clearly describe the method at all. This method section should be expanded.

A1.15: The "seasonal decompose analysis" is the original name of the method, which is always used to resolve long-term and repeated variation in term of years and seasonal variation. The two variation trends are similar to a combination of two filters with large and small bandwidth, which can be adjusted. Here we changed the "bandwidth" of the method by replacing seasonal variation with hour variation and replacing long-term variation in term of years with days. We reserved this expression of "seasonal decompose analysis" in the manuscript for its original application. To clarify this, we revised the sentence in line 400-403 of the main text:

"To elucidate this large uncertainty, a seasonal decomposition method (Hilas et al., 2006), which was performed by locally weighted linear regression to decompose the time series into three components, i.e., trend component, seasonal component and remainder, was applied (detailed process can be found in Text S4). By replacing

seasonal variation with hour variation, the method can down weight the impact of daily peak intensity variation."

In addition, we expanded the method section Text S4 in the supporting information to introduce more details about this method:

"A time series usually comprises three components: a long-term trend, seasonal fluctuation, and a remainder component (containing anything else in the time series). A long-term trend is a tendency or state of affairs in which a phenomenon develops and changes continuously over a longer period of time. Seasonal fluctuation is the regular variation caused by seasonal change. The time series decomposition can distill the component of repeatability from complex data. This method is similar to the combination of two filters with large and small bandwidth. The bandwidth can be adjusted for different time resolution. If an additive decomposition was assumed, the Eq. is:

$$y_t = S_t + T_t + R_t \quad \text{(S10)}$$

where y_t is the data, S_t is the seasonal fluctuation, T_t is the long-term trend, and R_t is the remainder component, all at period t. Taking 24 hours as the "season" in the calculation, i.e., adjusting the "bandwidth", we can get a clearer diurnal variation preventing the trend blurred by the varies intensity between days. The detailed process of the calculation applied in this paper can refer to Hilas et al. (2006)."

1.16. Line 340. For the strong BB emission period, are VOCs from BB considered in the calculation of OON production rate?

A1.16: The VOCs considered in the calculation of OON production rate are the same during the whole campaign, including the strong BB emission period here. VOCs from biomass burning emissions include alkanes, alkenes, aromatics (e.g., phenol and cresol), and terpenes (e.g., isoprene and monoterpenes) (Gilman et al. 2015;Liu et al. 2017). Thus, the calculation of OON production rate during the strong BB emission period shall include VOCs from biomass burning. To clarify this, we added brief discussion in line 370-372 of the main text:

"The precursors, e.g., alkanes, alkenes, aromatics (phenol and cresol), and terpenes (isoprene and monoterpenes), considered in the calculation were also contributed by biomass burning (Liu et al., 2017; Gilman et al., 2015), especially during the strong biomass burning emission period."

1.17. Line 413. Please rewrite this sentence because RO2+NO produces either RONO2 or O3.

A1.17: The sentence was revised in line 468-470:

"Fig. 6a shows a strong correlation between secondary gOON and O_x (R = 0.83, slope = 0.02 μg m^{-3}/ppb), which is within expectation as the major channel of gOON formation between peroxy radicals (RO_2) and NO can lead to the formation of ONs and O_3 by continual radical propagation and photolysis of NO_2 (Perring et al., 2013; Xu et al., 2021a)."

1.18. Figure S21. Please explain why ALWC (RH and others) is correlated with pOON/Ox, instead of pOON?

A1.18: The ALWC is correlated with "secondary pOON/O_x" ($pOON_{sec}/O_x$) as shown in Fig. S23 (original Fig. S21) in the revised supporting information. Using $pOON_{sec}/O_x$ instead of $pOON_{sec}$ was originated from Herndon et al. (2008) and Wood et al. (2010). Both studies showed that the observed [OOA]/[O_x] roughly serves as a useful tool to represent the calculated production of SOA vs production of O_x (P[SOA]/P[O_x]). As citated equation shown below:

$$\frac{\Delta[\mathrm{SOA}]}{\Delta[\mathrm{O_X}]} \approx \frac{P[\mathrm{SOA}]}{P[\mathrm{O_X}]}$$ (Wood et al., 2010)

In the recent studies, the variation of OOA/O_x ratios have been attributed to several factor including photochemical oxidation, heterogenous/aqueous reaction, and mixing with air aloft that contains residual SOA and O_x during boundary layer growth (Hu et al., 2016; Hayes et al., 2013; Nault et al., 2021). Nault et al. (2021) found the ratio of [OOA]/[O_x] is highly correlated with the BTEX fraction (Benzene, Toluene, Ethylbenzene and Xylene) in total measured VOCs among different urban areas across the world. Compared with short chain VOCs, the BTEX VOCs are more efficient to form SOA than O_x, resulting a higher OOA/O_x ratio. Multiple studies also found the OOA/O_x ratio also increases when there are heterogeneous/aqueous reactions which can lead to extra SOA formation but not O_x (Zhang et al., 2018; Zhan et al., 2021; Xu et al., 2017; Dai et al., 2019; Hu et al., 2016). In this study, we applied a similar concept of OOA/O_x to $pOON_{sec}/O_x$, since $pOON_{sec}$ is part of SOA.

The $pOON_{sec}/O_x$ ratios that positively correlated with ALWC and wet aerosol surface area suggested that the $pOON_{sec}$ formed by heterogenous/aqueous reaction partially account for the increasing ratio compared to gas-phase photochemistry (together with O_x formation). If absolute $pOON_{sec}$ instead of $pOON_{sec}/O_x$ was used, the correlation between RH (ALWC) and $pOON_{sec}$ would probably be influenced by meteorological factors (e.g., boundary layer height), introducing more ambiguity of the conclusion. Thus, the $pOON_{sec}/O_x$ instead of $pOON_{sec}$ was applied here. To clarify this, we added relative description and revised the caption of Figure S23:

"Figure S23. The ratio of Secondary (Sec.) pOON to Ox versus the (a) RH, (b) aerosol liquid water content (ALWC), (c) wet aerosol surface area, and (d) ambient temperature color-coded using the RH during the campaign. Regression slopes between pOON and Ox in photochemically processed urban emissions provide a metric to investigate the relative efficiency of pOON versus O_3 formation during photochemical oxidation (Wood et al., 2010; Hayes et al., 2013). The different values of secondary pOON/O_x ratio can be attributed to photochemical oxidation from different VOC constituent (Nault et al., 2021), heterogenous/aqueous reaction (Zhang et al., 2018; Zhan et al., 2021; Xu et al., 2017; Dai et al., 2019; Hu et al., 2016), and mixing with air aloft that contains residual pOON and O_x during boundary layer growth (Wood et al., 2010). The secondary pOON/O_x ratios that positive correlated with ALWC and wet aerosol surface area suggested that partial pOON might be formed by heterogenous/aqueous reaction, which can efficiently produce secondary pOON but inefficiently on O_x."

Reference

Andreae, M. O.: Soot Carbon and Excess Fine Potassium: Long-Range Transport of Combustion-Derived Aerosols, Science, 220, 1148-1151, https://doi.org/10.1126/science.220.4602.1148, 1983.

Ayres, B. R., Allen, H. M., Draper, D. C., Brown, S. S., Wild, R. J., Jimenez, J. L., Day, D. A., Campuzano-Jost, P., Hu, W., de Gouw, J., Koss, A., Cohen, R. C., Duffey, K. C., Romer, P., Baumann, K., Edgerton, E., Takahama, S., Thornton, J. A., Lee, B. H., Lopez-Hilfiker, F. D., Mohr, C., Wennberg, P. O., Nguyen, T. B., Teng, A., Goldstein, A. H., Olson, K., and Fry, J. L.: Organic nitrate aerosol formation via NO3+ biogenic volatile organic compounds in the southeastern United States, Atmos. Chem. Phys., 15, 13377-13392, https://doi.org/10.5194/acp-15-13377-2015, 2015.

Bhattarai, H., Saikawa, E., Wan, X., Zhu, H., Ram, K., Gao, S., Kang, S., Zhang, Q., Zhang, Y., Wu, G., Wang, X., Kawamura, K., Fu, P., and Cong, Z.: Levoglucosan as a tracer of biomass burning: Recent progress and perspectives, Atmospheric Research, 220, 20-33, https://doi.org/10.1016/j.atmosres.2019.01.004, 2019.

Bi, C., Krechmer, J. E., Frazier, G. O., Xu, W., Lambe, A. T., Claflin, M. S., Lerner, B. M., Jayne, J. T., Worsnop, D. R., Canagaratna, M. R., and Isaacman-VanWertz, G.: Coupling a gas chromatograph simultaneously to a flame ionization detector and chemical ionization mass spectrometer for isomer-resolved measurements of particle-phase organic compounds, Atmos. Meas. Tech., 14, 3895-3907, https://doi.org/10.5194/amt-14-3895-2021, 2021a.

Bi, C., Krechmer, J. E., Frazier, G. O., Xu, W., Lambe, A. T., Claflin, M. S., Lerner, B. M., Jayne, J. T., Worsnop, D. R., Canagaratna, M. R., and Isaacman-VanWertz, G.: Quantification of isomer-resolved iodide chemical ionization mass spectrometry sensitivity and uncertainty using a voltage-scanning approach, Atmos. Meas. Tech., 14, 6835-6850, https://doi.org/10.5194/amt-14-6835-2021, 2021b.

Chen, Y., Takeuchi, M., Nah, T., Xu, L., Canagaratna, M. R., Stark, H., Baumann, K., Canonaco, F., Prévôt, A. S. H., Huey, L. G., Weber, R. J., and Ng, N. L.: Chemical characterization of secondary organic aerosol at a rural site in the southeastern US: insights from simultaneous high-resolution time-of-flight aerosol mass spectrometer (HR-ToF-AMS) and FIGAERO chemical ionization mass spectrometer (CIMS) measurements, Atmos. Chem. Phys., 20, 8421-8440, https://doi.org/10.5194/acp-20-8421-2020, 2020.

Cubison, M. J., Ortega, A. M., Hayes, P. L., Farmer, D. K., Day, D., Lechner, M. J., Brune, W. H., Apel, E., Diskin, G. S., Fisher, J. A., Fuelberg, H. E., Hecobian, A., Knapp, D. J., Mikoviny, T., Riemer, D., Sachse, G. W., Sessions, W., Weber, R. J., Weinheimer, A. J., Wisthaler, A., and Jimenez, J. L.: Effects of aging on organic aerosol from open biomass burning smoke in aircraft and laboratory studies, Atmos. Chem. Phys., 11, 12049-12064, https://doi.org/10.5194/acp-11-12049-2011, 2011.

Dai, Q., Schulze, B. C., Bi, X., Bui, A. A. T., Guo, F., Wallace, H. W., Sanchez, N. P., Flynn, J. H., Lefer, B. L., Feng, Y., and Griffin, R. J.: Seasonal differences in formation processes of oxidized organic aerosol near Houston, TX, Atmos. Chem. Phys., 19, 9641-9661, 10.5194/acp-19-9641-2019, 2019.

Day, D. A., Liu, S., Russell, L. M., and Ziemann, P. J.: Organonitrate group concentrations in submicron particles with high nitrate and organic fractions in coastal southern California, Atmos. Environ., 44, 1970-1979, https://doi.org/10.1016/j.atmosenv.2010.02.045, 2010.

Day, D. A., Campuzano-Jost, P., Nault, B. A., Palm, B. B., Hu, W., Guo, H., Wooldridge, P. J., Cohen, R. C., Docherty, K. S., Huffman, J. A., de Sá, S. S., Martin, S. T., and Jimenez, J. L.: A systematic re-evaluation of methods for quantification of bulk particle-phase organic nitrates using real-time aerosol mass spectrometry, Atmos. Meas. Tech., 15, 459-483, https://doi.org/10.5194/amt-15-459-2022, 2022.

DeCarlo, P. F., Kimmel, J. R., Trimborn, A., Northway, M. J., Jayne, J. T., Aiken, A. C., Gonin, M., Fuhrer, K., Horvath, T., Docherty, K. S., Worsnop, D. R., and Jimenez, J. L.: Field-Deployable, High-Resolution, Time-of-Flight Aerosol Mass Spectrometer, Anal. Chem., 78, 8281-8289, https://doi.org/10.1021/ac061249n, 2006.

Farmer, D. K., Matsunaga, A., Docherty, K. S., Surratt, J. D., Seinfeld, J. H., Ziemann, P. J., and Jimenez, J. L.: Response of an aerosol mass spectrometer to organonitrates and organosulfates and implications for atmospheric chemistry, Proc. Natl. Acad. Sci. U. S. A., 107, 6670-6675, https://doi.org/10.1073/pnas.0912340107, 2010.

Fisher, J. A., Jacob, D. J., Travis, K. R., Kim, P. S., Marais, E. A., Miller, C. C., Yu, K., Zhu, L., Yantosca, R. M., Sulprizio, M. P., Mao, J., Wennberg, P. O., Crounse, J. D., Teng, A. P., Nguyen, T. B., St Clair, J. M., Cohen, R. C., Romer, P., Nault, B. A., Wooldridge, P. J., Jimenez, J. L., Campuzano-Jost, P., Day, D. A., Hu, W., Shepson, P. B., Xiong, F., Blake, D. R., Goldstein, A. H., Misztal, P. K., Hanisco, T. F., Wolfe, G. M., Ryerson, T. B., Wisthaler, A., and Mikoviny, T.: Organic nitrate chemistry and its implications for nitrogen budgets in an isoprene- and monoterpene-rich atmosphere: constraints from aircraft (SEAC(4)RS) and ground-based (SOAS) observations in the Southeast US, Atmos. Chem. Phys., 16, 5969-5991, https://doi.org/10.5194/acp-16-5969-2016, 2016.

Fry, J. L., Draper, D. C., Zarzana, K. J., Campuzano-Jost, P., Day, D. A., Jimenez, J. L., Brown, S. S., Cohen, R. C., Kaser, L., Hansel, A., Cappellin, L., Karl, T., Roux, A. H., Turnipseed, A., Cantrell, C., Lefer, B. L., and Grossberg, N.: Observations of gas- and aerosol-phase organic nitrates at BEACHON-RoMBAS 2011, Atmos. Chem. Phys., 13, 8585-8605, https://doi.org/10.5194/acp-13-8585-2013, 2013.

Gilman, J. B., Lerner, B. M., Kuster, W. C., Goldan, P. D., Warneke, C., Veres, P. R., Roberts, J. M., de Gouw, J. A., Burling, I. R., and Yokelson, R. J.: Biomass burning emissions and potential air quality impacts of volatile organic compounds and other trace gases from fuels common in the US, Atmos. Chem. Phys., 15, 13915-13938, https://doi.org/10.5194/acp-15-13915-2015, 2015.

Hamilton, J. F., Bryant, D. J., Edwards, P. M., Ouyang, B., Bannan, T. J., Mehra, A., Mayhew, A. W., Hopkins, J. R., Dunmore, R. E., Squires, F. A., Lee, J. D., Newland, M. J., Worrall, S. D., Bacak, A., Coe, H., Percival, C., Whalley, L. K., Heard, D. E., Slater, E. J., Jones, R. L., Cui, T., Surratt, J. D., Reeves, C. E., Mills, G. P., Grimmond, S., Sun, Y., Xu, W., Shi, Z., and Rickard, A. R.: Key Role of NO3 Radicals in the Production of Isoprene Nitrates and Nitrooxyorganosulfates in Beijing, Environ. Sci. Technol., 55, 842-853, https://doi.org/10.1021/acs.est.0c05689, 2021.

Hao, L. Q., Kortelainen, A., Romakkaniemi, S., Portin, H., Jaatinen, A., Leskinen, A., Komppula, M., Miettinen, P., Sueper, D., Pajunoja, A., Smith, J. N., Lehtinen, K. E. J., Worsnop, D. R., Laaksonen, A., and Virtanen, A.: Atmospheric submicron aerosol composition and particulate organic nitrate formation in a boreal forestland–urban mixed region, Atmos. Chem. Phys., 14, 13483-13495, https://doi.org/10.5194/acp-14-13483-2014, 2014.

Hayes, P. L., Ortega, A. M., Cubison, M. J., Froyd, K. D., Zhao, Y., Cliff, S. S., Hu, W. W., Toohey, D. W., Flynn, J. H., Lefer, B. L., Grossberg, N., Alvarez, S., Rappenglück, B., Taylor, J. W., Allan, J. D., Holloway, J. S., Gilman, J. B., Kuster, W. C., de Gouw, J. A., Massoli, P., Zhang, X., Liu, J., Weber, R. J., Corrigan, A. L., Russell, L. M., Isaacman, G., Worton, D. R., Kreisberg, N. M., Goldstein, A. H., Thalman, R., Waxman, E. M., Volkamer, R., Lin, Y. H., Surratt, J. D., Kleindienst, T. E., Offenberg, J. H., Dusanter, S., Griffith, S., Stevens, P. S., Brioude, J., Angevine, W. M., and Jimenez, J. L.: Organic aerosol composition and sources in Pasadena, California, during the 2010 CalNex campaign, J. Geophys. Res.: Atmos., 118, 9233-9257, 10.1002/jgrd.50530, 2013.

Herndon, S. C., Onasch, T. B., Wood, E. C., Kroll, J. H., Canagaratna, M. R., Jayne, J. T., Zavala, M. A., Knighton, W. B., Mazzoleni, C., Dubey, M. K., Ulbrich, I. M., Jimenez, J. L., Seila, R., de Gouw, J. A., de Foy, B., Fast, J., Molina, L. T., Kolb, C. E., and Worsnop, D. R.: Correlation of secondary organic aerosol with odd oxygen in Mexico City, Geophys. Res. Lett., 35, https://doi.org/10.1029/2008GL034058, 2008.

Hilas, C. S., Goudos, S. K., and Sahalos, J. N.: Seasonal decomposition and forecasting of telecommunication data: A comparative case study, Technological Forecasting and Social Change, 73, 495-509, https://doi.org/10.1016/j.techfore.2005.07.002, 2006.

Ho, K. F., Engling, G., Ho, S. S. H., Huang, R., Lai, S., Cao, J., and Lee, S. C.: Seasonal variations of anhydrosugars in PM2.5 in the Pearl River Delta Region, China, Tellus B: Chemical and Physical Meteorology, 66, 10.3402/tellusb.v66.22577, 2014.

Hu, W., Hu, M., Hu, W., Jimenez, J. L., Yuan, B., Chen, W., Wang, M., Wu, Y., Chen, C., Wang, Z., Peng, J., Zeng, L., and Shao, M.: Chemical composition, sources, and aging process of submicron aerosols in Beijing: Contrast between summer and winter, J. Geophys. Res.: Atmos., 121, 1955-1977, 10.1002/2015jd024020, 2016.

Huang, W., Saathoff, H., Shen, X., Ramisetty, R., Leisner, T., and Mohr, C.: Chemical Characterization of Highly Functionalized Organonitrates Contributing to Night-Time Organic Aerosol Mass Loadings and Particle Growth, Environ. Sci. Technol., 53, 1165-1174, https://doi.org/10.1021/acs.est.8b05826, 2019.

Isaacman-VanWertz, G., Massoli, P., O'Brien, R., Lim, C., Franklin, J. P., Moss, J. A., Hunter, J. F., Nowak, J. B., Canagaratna, M. R., Misztal, P. K., Arata, C., Roscioli, J. R., Herndon, S. T., Onasch, T. B., Lambe, A. T., Jayne, J. T., Su, L., Knopf, D. A., Goldstein, A. H., Worsnop, D. R., and Kroll, J. H.: Chemical evolution of atmospheric organic carbon over multiple generations of oxidation, Nature Chemistry, 10, 462-468, https://doi.org/10.1038/s41557-018-0002-2, 2018.

Iyer, S., Lopez-Hilfiker, F., Lee, B. H., Thornton, J. A., and Kurtén, T.: Modeling the Detection of Organic and Inorganic Compounds Using Iodide-Based Chemical Ionization, The Journal of Physical Chemistry A, 120, 576-587, https://doi.org/10.1021/acs.jpca.5b09837, 2016.

Jiang, F., Liu, J., Cheng, Z., Ding, P., Zhu, S., Yuan, X., Chen, W., Zhang, Z., Zong, Z., Tian, C., Hu, W., Zheng, J., Szidat, S., Li, J., and Zhang, G.: Quantitative evaluation for the sources and aging processes of organic aerosols in urban Guangzhou: Insights from a comprehensive method of dual-carbon isotopes and macro tracers, Sci Total Environ, 164182, https://doi.org/10.1016/j.scitotenv.2023.164182, 2023.

Kiendler-Scharr, A., Mensah, A. A., Friese, E., Topping, D., Nemitz, E., Prevot, A. S. H., Äijälä, M., Allan, J., Canonaco, F., Canagaratna, M., Carbone, S., Crippa, M., Dall Osto, M., Day, D. A., De Carlo, P., Di Marco, C. F., Elbern, H., Eriksson, A., Freney, E., Hao, L., Herrmann, H., Hildebrandt, L., Hillamo, R., Jimenez, J. L., Laaksonen, A., McFiggans, G., Mohr, C., O'Dowd, C., Otjes, R., Ovadnevaite, J., Pandis, S. N., Poulain, L., Schlag, P., Sellegri, K., Swietlicki, E., Tiitta, P., Vermeulen, A., Wahner, A., Worsnop, D., and Wu, H. C.: Ubiquity of organic nitrates from nighttime chemistry in the European submicron aerosol, Geophys. Res. Lett., 43, 7735-7744, https://doi.org/10.1002/2016gl069239, 2016.

Lanz, V. A., Prévôt, A. S. H., Alfarra, M. R., Weimer, S., Mohr, C., DeCarlo, P. F., Gianini, M. F. D., Hueglin, C., Schneider, J., Favez, O., D'Anna, B., George, C., and Baltensperger, U.: Characterization of aerosol chemical composition with aerosol mass spectrometry in Central Europe: an overview, Atmos. Chem. Phys., 10, 10453-10471, https://doi.org/10.5194/acp-10-10453-2010, 2010.

Lee, A. K. Y., Adam, M. G., Liggio, J., Li, S.-M., Li, K., Willis, M. D., Abbatt, J. P. D., Tokarek, T. W., Odame-Ankrah, C. A., Osthoff, H. D., Strawbridge, K., and Brook, J. R.: A large contribution of anthropogenic organo-nitrates to secondary organic aerosol in the Alberta oil sands, Atmos. Chem. Phys., 19, 12209-12219, https://doi.org/10.5194/acp-19-12209-2019, 2019.

Lee, B. H., Lopez-Hilfiker, F. D., D'Ambro, E. L., Zhou, P., Boy, M., Petäjä, T., Hao, L., Virtanen, A., and Thornton, J. A.: Semi-volatile and highly oxygenated gaseous and particulate organic compounds observed above a boreal forest canopy, Atmos. Chem. Phys., 18, 11547-11562, https://doi.org/10.5194/acp-18-11547-2018, 2018.

Lee, B. H., Mohr, C., Lopez-Hilfiker, F. D., Lutz, A., Hallquist, M., Lee, L., Romer, P., Cohen, R. C., Iyer, S., Kurten, T., Hu, W., Day, D. A., Campuzano-Jost, P., Jimenez, J. L., Xu, L., Ng, N. L., Guo, H., Weber, R. J., Wild, R. J., Brown, S. S., Koss, A., de Gouw, J., Olson, K., Goldstein, A. H., Seco, R., Kim, S., McAvey, K., Shepson, P. B., Starn, T., Baumann, K., Edgerton, E. S., Liu, J., Shilling, J. E., Miller, D. O., Brune, W., Schobesberger, S., D'Ambro, E. L., and Thornton, J. A.: Highly functionalized organic nitrates in the southeast United States: Contribution to secondary organic aerosol and reactive nitrogen budgets, Proc. Natl. Acad. Sci. U. S. A., 113, 1516-1521, https://doi.org/10.1073/pnas.1508108113, 2016.

Li, C., Wang, H., Chen, X., Zhai, T., Ma, X., Yang, X., Chen, S., Li, X., Zeng, L., and Lu, K.: Observation and modeling of organic nitrates on a suburban site in southwest China, Sci. Total Environ., 859, 160287, https://doi.org/10.1016/j.scitotenv.2022.160287, 2023.

Liebmann, J., Sobanski, N., Schuladen, J., Karu, E., Hellén, H., Hakola, H., Zha, Q., Ehn, M., Riva, M., Heikkinen, L., Williams, J., Fischer, H., Lelieveld, J., and Crowley, J. N.: Alkyl nitrates in the boreal forest: formation via the NO3-, OH- and O3 induced oxidation of biogenic volatile organic compounds and ambient lifetimes, Atmos. Chem. Phys., 19, 10391-10403, https://doi.org/10.5194/acp-19-10391-2019, 2019.

Liu, X., Huey, L. G., Yokelson, R. J., Selimovic, V., Simpson, I. J., Müller, M., Jimenez, J. L., Campuzano-Jost, P., Beyersdorf, A. J., Blake, D. R., Butterfield, Z., Choi, Y., Crounse, J. D., Day, D. A., Diskin, G. S., Dubey, M. K., Fortner, E., Hanisco, T. F., Hu, W., King, L. E., Kleinman, L., Meinardi, S., Mikoviny, T., Onasch, T. B., Palm, B. B., Peischl, J., Pollack, I. B., Ryerson, T. B., Sachse, G. W., Sedlacek, A. J., Shilling, J. E., Springston, S., St. Clair, J. M., Tanner, D. J., Teng, A. P., Wennberg, P. O., Wisthaler, A., and Wolfe, G. M.: Airborne measurements of western U.S. wildfire emissions: Comparison with prescribed burning and air quality implications, J. Geophys. Res.: Atmos., 122, 6108-6129, https://doi.org/10.1002/2016jd026315, 2017.

Lopez-Hilfiker, F. D., Iyer, S., Mohr, C., Lee, B. H., D'Ambro, E. L., Kurtén, T., and Thornton, J. A.: Constraining the sensitivity of iodide adduct chemical ionization mass spectrometry to multifunctional organic molecules using the collision limit and thermodynamic stability of iodide ion adducts, Atmos. Meas. Tech., 9, 1505-1512, https://doi.org/10.5194/amt-9-1505-2016, 2016.

Mao, S., Li, J., Cheng, Z., Zhong, G., Li, K., Liu, X., and Zhang, G.: Contribution of Biomass Burning to Ambient Particulate Polycyclic Aromatic Hydrocarbons at a Regional Background Site in East China, Environmental Science & Technology Letters, 5, 56-61, 10.1021/acs.estlett.8b00001, 2018.

Müller, S., Giorio, C., and Borduas-Dedekind, N.: Tracking the Photomineralization Mechanism in Irradiated Lab-Generated and Field-Collected Brown Carbon Samples and Its Effect on Cloud Condensation Nuclei Abilities, ACS Environmental Au, 10.1021/acsenvironau.2c00055, 2023.

Nault, B. A., Jo, D. S., McDonald, B. C., Campuzano-Jost, P., Day, D. A., Hu, W., Schroder, J. C., Allan, J., Blake, D. R., Canagaratna, M. R., Coe, H., Coggon, M. M., DeCarlo, P. F., Diskin, G. S., Dunmore, R., Flocke, F., Fried, A., Gilman, J. B., Gkatzelis, G., Hamilton, J. F., Hanisco, T. F., Hayes, P. L., Henze, D. K., Hodzic, A., Hopkins, J., Hu, M., Huey, L. G., Jobson, B. T., Kuster, W. C., Lewis, A., Li, M., Liao, J., Nawaz, M. O., Pollack, I. B., Peischl, J., Rappenglück, B., Reeves, C. E., Richter, D., Roberts, J. M., Ryerson, T. B., Shao, M., Sommers, J. M., Walega, J., Warneke, C., Weibring, P., Wolfe, G. M., Young, D. E., Yuan, B., Zhang, Q., de Gouw, J. A., and Jimenez, J. L.: Secondary organic aerosols from anthropogenic volatile organic compounds contribute substantially to air pollution mortality, Atmos. Chem. Phys., 21, 11201-11224, 10.5194/acp-21-11201-2021, 2021.

Perring, A. E., Pusede, S. E., and Cohen, R. C.: An observational perspective on the atmospheric impacts of alkyl and multifunctional nitrates on ozone and secondary organic aerosol, Chem. Rev., 113, 5848-5870, https://doi.org/10.1021/cr300520x, 2013.

Pye, H. O., Luecken, D. J., Xu, L., Boyd, C. M., Ng, N. L., Baker, K. R., Ayres, B. R., Bash, J. O., Baumann, K., Carter, W. P., Edgerton, E., Fry, J. L., Hutzell, W. T., Schwede, D. B., and Shepson, P. B.: Modeling the Current and Future Roles of Particulate Organic Nitrates in the Southeastern United States, Environ. Sci. Technol., 49, 14195-14203, https://doi.org/10.1021/acs.est.5b03738, 2015.

Robinson, M. A., Neuman, J. A., Huey, L. G., Roberts, J. M., Brown, S. S., and Veres, P. R.: Temperature-dependent sensitivity of iodide chemical ionization mass spectrometers, Atmos. Meas. Tech., 15, 4295-4305, https://doi.org/10.5194/amt-15-4295-2022, 2022.

Rollins, A. W., Browne, E. C., Min, K. E., Pusede, S. E., Wooldridge, P. J., Gentner, D. R., Goldstein, A. H., Liu, S., Day, D. A., Russell, L. M., and Cohen, R. C.: Evidence for NO(x) control over nighttime SOA formation, Science, 337, 1210-1212, https://doi.org/10.1126/science.1221520, 2012.

Salvador, C. M., Chou, C. C. K., Cheung, H. C., Ho, T. T., Tsai, C. Y., Tsao, T. M., Tsai, M. J., and Su, T. C.: Measurements of submicron organonitrate particles: Implications for the impacts of NOx pollution in a subtropical forest, Atmospheric Research, 245, https://doi.org/10.1016/j.atmosres.2020.105080, 2020.

Singla, V., Mukherjee, S., Pandithurai, G., Dani, K. K., and Safai, P. D.: Evidence of Organonitrate Formation at a High Altitude Site, Mahabaleshwar, during the Pre-monsoon Season, Aerosol and Air Quality Research, 19, 1241-1251, https://doi.org/10.4209/aaqr.2018.03.0110, 2019.

Sobanski, N., Thieser, J., Schuladen, J., Sauvage, C., Song, W., Williams, J., Lelieveld, J., and Crowley, J. N.: Day and night-time formation of organic nitrates at a forested mountain site in south-west Germany, Atmos. Chem. Phys., 17, 4115-4130, https://doi.org/10.5194/acp-17-4115-2017, 2017.

Takeuchi, M. and Ng, N. L.: Chemical composition and hydrolysis of organic nitrate aerosol formed from hydroxyl and nitrate radical oxidation of α-pinene and β-pinene, Atmos. Chem. Phys., 19, 12749-12766, https://doi.org/10.5194/acp-19-12749-2019, 2019.

Urban, R. C., Lima-Souza, M., Caetano-Silva, L., Queiroz, M. E. C., Nogueira, R. F. P., Allen, A. G., Cardoso, A. A., Held, G., and Campos, M. L. A. M.: Use of levoglucosan, potassium, and water-soluble organic carbon to characterize the origins of biomass-burning aerosols, Atmos. Environ., 61, 562-569, https://doi.org/10.1016/j.atmosenv.2012.07.082, 2012.

Wang, X., Shen, Z., Liu, F., Lu, D., Tao, J., Lei, Y., Zhang, Q., Zeng, Y., Xu, H., Wu, Y., Zhang, R., and Cao, J.: Saccharides in summer and winter PM2.5 over Xi'an, Northwestern China: Sources, and yearly variations of biomass burning contribution to PM2.5, Atmospheric Research, 214, 410-417, 10.1016/j.atmosres.2018.08.024, 2018.

Wang, Y., Hu, M., Lin, P., Guo, Q., Wu, Z., Li, M., Zeng, L., Song, Y., Zeng, L., Wu, Y., Guo, S., Huang, X., and He, L.: Molecular Characterization of Nitrogen-Containing Organic Compounds in Humic-like Substances Emitted from Straw Residue Burning, Environ. Sci. Technol., 51, 5951-5961, https://doi.org/10.1021/acs.est.7b00248, 2017.

Wood, E. C., Canagaratna, M. R., Herndon, S. C., Onasch, T. B., Kolb, C. E., Worsnop, D. R., Kroll, J. H., Knighton, W. B., Seila, R., Zavala, M., Molina, L. T., DeCarlo, P. F., Jimenez, J. L., Weinheimer, A. J., Knapp, D. J., Jobson, B. T., Stutz, J., Kuster, W. C., and Williams, E. J.: Investigation of the correlation between odd oxygen and secondary organic aerosol in Mexico City and Houston, Atmos. Chem. Phys., 10, 8947-8968, 10.5194/acp-10-8947-2010, 2010.

Xu, L., Suresh, S., Guo, H., Weber, R. J., and Ng, N. L.: Aerosol characterization over the southeastern United States using high-resolution aerosol mass spectrometry: spatial and seasonal variation of aerosol composition and sources with a focus on organic nitrates, Atmos. Chem. Phys., 15, 7307-7336, https://doi.org/10.5194/acp-15-7307-2015, 2015.

Xu, L., Crounse, J. D., Vasquez, K. T., Allen, H., Wennberg, P. O., Bourgeois, I., Brown, S. S., Campuzano-Jost, P., Coggon, M. M., Crawford, J. H., DiGangi, J. P., Diskin, G. S., Fried, A., Gargulinski, E. M., Gilman, J. B., Gkatzelis, G.

I., Guo, H., Hair, J. W., Hall, S. R., Halliday, H. A., Hanisco, T. F., Hannun, R. A., Holmes, C. D., Huey, L. G., Jimenez, J. L., Lamplugh, A., Lee, Y. R., Liao, J., Lindaas, J., Neuman, J. A., Nowak, J. B., Peischl, J., Peterson, D. A., Piel, F., Richter, D., Rickly, P. S., Robinson, M. A., Rollins, A. W., Ryerson, T. B., Sekimoto, K., Selimovic, V., Shingler, T., Soja, A. J., St. Clair, J. M., Tanner, D. J., Ullmann, K., Veres, P. R., Walega, J., Warneke, C., Washenfelder, R. A., Weibring, P., Wisthaler, A., Wolfe, G. M., Womack, C. C., and Yokelson, R. J.: Ozone chemistry in western U.S. wildfire plumes, Sci. Adv., 7, eabl3648, https://doi.org/10.1126/sciadv.abl3648, 2021a.

Xu, W., Takeuchi, M., Chen, C., Qiu, Y., Xie, C., Xu, W., Ma, N., Worsnop, D. R., Ng, N. L., and Sun, Y.: Estimation of particulate organic nitrates from thermodenuder–aerosol mass spectrometer measurements in the North China Plain, Atmos. Meas. Tech., 14, 3693-3705, https://doi.org/10.5194/amt-14-3693-2021, 2021b.

Xu, W., Han, T., Du, W., Wang, Q., Chen, C., Zhao, J., Zhang, Y., Li, J., Fu, P., Wang, Z., Worsnop, D. R., and Sun, Y.: Effects of Aqueous-Phase and Photochemical Processing on Secondary Organic Aerosol Formation and Evolution in Beijing, China, Environ. Sci. Technol., 51, 762-770, 10.1021/acs.est.6b04498, 2017.

Ye, C., Yuan, B., Lin, Y., Wang, Z., Hu, W., Li, T., Chen, W., Wu, C., Wang, C., Huang, S., Qi, J., Wang, B., Wang, C., Song, W., Wang, X., Zheng, E., Krechmer, J. E., Ye, P., Zhang, Z., Wang, X., Worsnop, D. R., and Shao, M.: Chemical characterization of oxygenated organic compounds in the gas phase and particle phase using iodide CIMS with FIGAERO in urban air, Atmos. Chem. Phys., 21, 8455-8478, https://doi.org/10.5194/acp-21-8455-2021, 2021.

Yu, K., Zhu, Q., Du, K., and Huang, X.-F.: Characterization of nighttime formation of particulate organic nitrates based on high-resolution aerosol mass spectrometry in an urban atmosphere in China, Atmos. Chem. Phys., 19, 5235-5249, https://doi.org/10.5194/acp-19-5235-2019, 2019.

Zhan, B., Zhong, H., Chen, H., Chen, Y., Li, X., Wang, L., Wang, X., Mu, Y., Huang, R.-J., George, C., and Chen, J.: The roles of aqueous-phase chemistry and photochemical oxidation in oxygenated organic aerosols formation, Atmos. Environ., 266, 118738, https://doi.org/10.1016/j.atmosenv.2021.118738, 2021.

Zhang, C., Lu, X., Zhai, J., Chen, H., Yang, X., Zhang, Q., Zhao, Q., Fu, Q., Sha, F., and Jin, J.: Insights into the formation of secondary organic carbon in the summertime in urban Shanghai, JEnvS, 72, 118-132, https://doi.org/10.1016/j.jes.2017.12.018, 2018.

Zhu, H.-X., Tao, X.-M., Wang, C., Zhang, L.-L., and Zheng, X.-Y.: Spatial and Temporal Distribution Characteristics of Levoglucosan and Its Isomers in PM2.5 in Beijing and Six Surrounding Cities, Environmental Science, 41, 1544-1549, 10.13227/j.hjkx.201906029, 2020.